Vol. 117: 205–214, 2016
doi: 10.3354/dao02943

DISEASES OF AQUATIC ORGANISMS
Dis Aquat Org

Published January 13

Genotoxic effects and gene expression changes in larval zebrafish after exposure to $ZnCl_2$ and ZnO nanoparticles

Halis Boran*, Gokay Ulutas

Recep Tayyip Erdoğan University, Faculty of Fisheries, 53100 Rize, Turkey

ABSTRACT: Engineered nanoparticles (NPs) can potentially generate adverse effects at the tissue, organ, cellular, subcellular, DNA, and protein levels due to their unique physico-chemical properties. Dissoluble NPs (e.g. nZnO) can be toxic in aquatic organisms. We compared effects of nZnO and corresponding concentrations of released Zn(II) by water-soluble $ZnCl_2$ on larval zebrafish *Danio rerio* (72 h post fertilization) by analyzing changes in expression levels of stress-related genes (*p53*, *rad51*, *mt2*) by qRT-PCR. Additionally, genotoxicity of nZnO and Zn(II) was assessed. The lethal concentrations for 50% mortality (LC_{50}) in larval zebrafish exposed for 96 h to 0 to 70 mg l^{-1} nZnO and Zn(II) were 21.37 ± 1.81 mg l^{-1} (95% CI) and 4.66 ± 0.11 mg l^{-1}, respectively. A concentration-dependent increase in DNA strand breaks was detected in cells from larvae exposed (96 h) to nZnO and Zn(II). DNA damage was higher in Zn(II)- than nZnO-exposed larvae. Induction of stress-related genes in larvae was complex and was not directly related to nZnO and Zn(II) concentrations, although there was significant induction in the *mt2* gene of larvae exposed to Zn(II) and nZnO relative to controls. *mt2* induction of 20.5 ± 1.9-fold and 2.5 ± 0.8-fold change (mean ± SEM) was observed in larvae at the highest Zn(II) and nZnO concentrations (3 and 6 mg l^{-1}), respectively. The results suggest that toxicity associated with nZnO is primarily due to the release of Zn(II).

KEY WORDS: Nanoscale ZnO · Zinc chloride · Genotoxicity · Stress-related genes · *Danio rerio*

INTRODUCTION

Metallic nanoparticles (NPs) are increasingly applied in materials, cosmetics, and technical applications, and metal oxides are the most widely used engineered nanomaterials (US EPA 2007). Among the various engineered nanomaterials, zinc oxide NPs (nZnO) are widely used all over the world, especially in semiconductors, solar panel devices, personal care products, paints, plastics, ceramics, glass, cement, rubber, pigments, and even in waste water treatment (Gottschalk et al. 2009, Zimmermann et al. 2012, Ma et al. 2013). Consequently, there is the high potential for release into the environment during production, use, and disposal.

NPs may have different physico-chemical properties or behaviors in contrast to bulk materials, making prediction of their fate challenging (Li et al. 2014). Their state of aggregation, and consequently their settling into sediments, depends on surface properties, abiotic factors, and the presence of dissolved organic matter in surrounding media (Zhou & Keller 2010, Shaw & Handy 2011). Most NPs in aquatic environments are covered by adsorbed layers of natural organic material, such as humic substances and polysaccharides, which can influence stability of inorganic NP suspensions (Hyung et al. 2007) and provide potential binding sites for trace elements (Buffle et al. 1990).

The divalent ion forms of Zn are nutritionally essential for all living organisms, as Zn is a co-factor

*Corresponding author: halis.boran@erdogan.edu.tr

for a number of enzymes. However, when present in excessive concentrations, this metal can cause adverse effects (Regoli & Principato 1995, Wilson et al. 2012). nZnO can partially but relatively rapidly dissolve in water, and the release of free Zn ions is the primary source of toxicity (Franklin et al. 2007, Blinova et al. 2010, Buerki-Thurnherr et al. 2013). Several studies have indicated that nZnO are toxic to fish: mortality, hatching inhibition, retarded growth, tissue injuries, and malformation have been reported in embryonic and larval zebrafish *Danio rerio* exposed to nZnO (Zhu et al. 2009, Bai et al. 2010, Zhao et al. 2013). Although some studies found that toxicity of nZnO could be mainly attributed to dissolved Zn ions (Franklin et al. 2007, Wong et al. 2010), toxicity of nZnO cannot always be explained by the dissolved Zn ions (Bai et al. 2010, Yu et al. 2011).

Particle-induced generation of reactive oxygen species (ROS) and dissolution to ionic Zn represent the primary modes of action for nZnO toxicity across all species tested (Ma et al. 2013). Indeed, ROS induction triggering an oxidative stress response has become a widely accepted paradigm for cellular effects of NPs (Nel et al. 2006, Zhu et al. 2009, Song et al. 2010, Sharma et al. 2012). Excessive production of ROS can induce pro-inflammatory and cytotoxic effects (Nel et al. 2006). nZnO and associated released Zn(II) may ultimately lead to apoptosis (Buerki-Thurnherr et al. 2013) and acute toxicity at high concentrations. Therefore, toxicity of nZnO may involve a combination of these 2 mechanisms. Thus, there are conflicting observations, and further research is needed to explain these contradictions.

In the present study, we contrast effects of nZnO and corresponding concentrations of released Zn(II) (derived from $ZnCl_2$) in experimental exposures of larval zebrafish in environmentally relevant media. The objectives of our present study were to (1) compare the acute toxicity of nZnO and Zn(II); (2) assess the effects of nZnO and Zn(II) on the expression of target genes including stress-related genes; and (3) determine the DNA damage of nZnO and Zn(II) using the comet assay.

MATERIALS AND METHODS

Experimental fish

Broodstock zebrafish *Danio rerio* (age 6–7 mo) were reared in closed-loop recirculation aquaria systems within the Zebrafish Research Facility at Recep Tayyip Erdoğan University, and maintained under routine approved animal welfare protocols. Photoperiod was 14:10 h (light:dark), and fish were fed 3 times daily with dry fish flakes (TetraMin) or live brine shrimp nauplii (*Artemia* sp.). Fish were bulk spawned, and eggs were collected and reared in 50 ml petri dishes with daily water changes. After hatching, the larvae were inspected and small or malformed larvae were removed. Hatched larvae (72 h post fertilization, hpf) were used for all exposures. Local (Rize, Turkey) mains supply water maintained at 27 ± 1°C was obtained. The water was left to stand for a minimum of 24 h and aerated to expel any chlorine. This water was used for all larval exposures. Water quality criteria were measured daily (mean ± SD) for pH (7.1 ± 0.4), temperature (27 ± 1°C), and dissolved oxygen (93% ± 2), and nitrite (<0.1 mg l^{-1}), nitrate (<0.02 mg l^{-1}), and ammonium (<20 mg l^{-1}) were measured weekly.

Experimental design and physicochemical analyses

Dry and powdered nZnO, obtained from Sigma Aldrich, contained at least 80% Zn by weight, an average particle size of <100 nm, and a specific surface area of 25 ± 7 m^2 g^{-1}. A 1 mg ml^{-1} stock solution of nZnO was generated without solvents by dispersing the NPs in ultrapure Milli-Q (Millipore) water with sonication (bath-type sonicator, 35 kHz frequency, Jeio Tech UC-20) for 1 h. Pure (97%) $ZnCl_2$ (MW 136.28) was obtained from Mediko Kimya. The Zn salt was dissolved in ultrapure Milli-Q water to produce a stock solution (1 mg ml^{-1}) from which working concentration solutions were prepared by further dilution with Milli-Q water. The 2 l test chambers developed in previous studies (Boran et al. 2012, Boyle et al. 2015) were used to provide homogeneous dispersions of NP-containing water to zebrafish larvae held in a semi-isolated plastic pipe suspended in the middle third of the water column. nZnO exposures were performed using these chambers, and Zn(II) exposures were performed using a 400 ml static beaker with dechlorinated tap water. To confirm appropriate sublethal concentrations for larval zebrafish exposure to Zn(II) and nZnO, the 96 h mortality of larvae (n = 30 per beaker) was measured at 7 concentrations (0, 1, 5, 10, 20, 40, and 70 mg l^{-1}) with replicate concentrations (n = 3 total per concentration) run on separate occasions. Mortality after 96 h exposure was recorded, and the concentration of Zn resulting in 50% mortality (LC_{50}) was computed by probit analysis and compared between nZnO and

Zn(II). In DNA damage and gene expression analyses, sublethal concentrations of Zn(II) (0, 0.1, 0.5, 1, 2, and 3 mg l^{-1}) and nZnO (0, 0.2, 1, 2, 4, and 6 mg l^{-1}) were used for 96 h exposures.

A scanning electron microscope (SEM; JSM-6610, JEOL) was used to characterize the morphology of nZnO. The working distance was set at 12 mm, and an acceleration voltage of 20 kV was used. Characterization of nZnO in the aqueous phase was conducted by NP tracking analysis (NTA) with a Malvern Zetasizer Nano ZSP (Malvern Instruments) particle analyzer. The 2 l preparations (i.e. 1 mg l^{-1} nZnO in 2 l fish water stirred for 96 h) were evaluated. The nZnO solutions were prepared and samples were collected from the middle of the water column and analyzed immediately after collection. The samples were collected after 0, 4, 24, 48, 72, and 96 h of stirring to compare changes in particle size and number over time during sedimentation of the nZnO. At each time point, 3 independent samples were collected from the nZnO solution, and mean particle size distribution plots were computed. The ability of the chambers to maintain nZnO in suspension was analyzed by inductively coupled plasma optical emission spectrometer (ICP-OES, Perkin Elmer Optima 7000 DV). After dosing the chambers with nZnO, 10 ml water samples were taken immediately (0 h) from within the 15 ml Falcon tube and acidified with nitric acid (trace element grade, Fisher Scientific). Additional samples were taken during the time course of the 96 h exposure, acidified, and analyzed for Zn concentrations against matrix-matched acidified element standards. Also, the concentration of soluble Zn was measured by ICP-OES. To completely remove the particulate Zn, after the dispersion was allowed to stand for 96 h, 10 ml of the dispersion were applied to the ultrafiltration membrane (molecular weight cutoff was 50 000: Vivaspin 20-50 k, GE Healthcare) and centrifuged at 6000 × *g* (60 min). The membrane was washed 3 times with 5 ml of Milli-Q water, and the amount of Zn in the filtrate was measured by ICP-OES.

Table 1. Zebrafish *Danio rerio* gene-specific primer sequences

Gene	Primer	Nucleotide sequence (5′–3′)	Product size (bp)
p53	Forward	TTG TCC CAT ATG AAG CAC CA	200
	Reverse	TTT CCT GTC TCT GCC TGG AC	
rad51	Forward	ACT AGC CGT CAC CTG CCA GC	133
	Reverse	ACT GCC CAC CAG ACC ATA CCG TT	
mt2	Forward	CTG CGA ATG TGC CAA GAC TGG AAC	243
	Reverse	GCG ATG CAA AAC GCA GAC GT	
β-*actin*	Forward	ACA CAG CCA TGG ATG AGG AAA TCG	138
	Reverse	TCA CTC CCT GAT GTC TGG GTC GT	

Gene expression analyses

Total RNA was extracted from the samples of 30 larvae, mechanically homogenized in Buffer RLT (Qiagen) and frozen at –80°C, using the RNeasy MiniKit for animal tissue (Qiagen) and following the manufacturer's protocol, with initial sonication (3–5 s) in RLT-homogenized samples, additional tissue break-up with a QiaShredder column, and a 15 min DNase treatment. RNA was eluted into 30 µl, and the concentration and quality of total RNA were determined with a spectrophotometer (NanoDrop, ND-2000 Spectrophotometer, Thermo Scientific). All samples were diluted to 100 ng $µl^{-1}$ total RNA, and 800 ng were used to synthesize cDNA following the manufacturer's protocol for the ImProm-II™ Reverse Transcription System (Promega), with hexanucleotide primers and deoxynucleotide mix (Sigma-Aldrich). cDNA was synthesized under the following conditions: annealing at 25°C, extension at 42°C, and heat-inactivation of transcriptase at 70°C (T100™ Thermal Cycler, Bio-Rad). cDNA was stored at –80°C until q-RT-PCR gene expression analysis.

Primers specific for zebrafish *rad51* (NCBI Reference Sequence: NM_2013206), *p53* (NM_131327.1), and *mt2* (NM_001131053.2) genes and the zebrafish housekeeping gene β-*actin* (NM_131031.1) were obtained from Bio Basic (Table 1). In accordance with the manufacturer's instructions, the lyophilized primers were reconstituted to 100 µmol with RNase-free water and mixed with SYBR Green JumpStart *Taq* ReadyMix to give a final reaction concentration of 375 nmol in 20 µl total volume. Standard PCR was performed using a cDNA sample dilution series with target gene primers, and the product was assessed for size, band strength, and purity by gel electrophoresis using a 1% agarose gel.

Real-time fluorescence was detected (Rotor-Gene RG-3000 Real-Time Thermal Cycler, Corbett Research) over 40 cycles, with cycling conditions of 94°C for denaturing, primer-specific annealing at 55–60°C, and extension at 72°C. The melt curve was

analyzed from the following conditions: 15 s at 94°C, 1 min at 60°C, and 15 s at 94°C. For analysis, the cycle threshold was set to 0.5 for all qPCR runs. A standard curve of cDNA template (pooled template from each sample within an experiment), was run in each reaction to allow for within-experiment reaction normalization.

For gene expression analysis, the efficiency (E) of qRT-PCR was calculated as

$$E = 10^{\left(-\frac{1}{slope}\right)} - 1 \quad (1)$$

based on a 4- or 5-point standard curve in each reaction. Samples from the same experiment run in multiple reactions were normalized to the reaction with the efficiency closest to 1 by adjusting for slope and intercept of the standard curves. Efficiencies between 0.9 and 1.1 were accepted for further analyses, and the comparative quantification method ($2^{-\Delta\Delta Ct}$; Pfaffl 2001) was used for calculating fold-changes in the gene of interest normalized to β-*actin*.

Single cell gel electrophoresis for detecting DNA damage

A comet assay was carried out following routine procedures (Reinardy et al. 2013), with some modifications. In brief, after a 96 h sublethal exposure to nZnO and Zn(II), zebrafish larvae (n = 40 for each concentration) were mechanically homogenized (Pellet pestles, cordless motor, Sigma) in lysis buffer (RLT buffer, Qiagen RNeasy MiniKit) and centrifuged for 15 s at 8000 × *g*. The supernatant was removed, and 10 µl of re-suspended cells were mixed with 180 µl of low-melting-point agarose (0.5%), dropped onto a slide pre-coated with 1.5% normal melting point agarose (dried overnight), and flattened with coverslips. For the positive control, after embedding control larvae cells on agarose, 50 µl of 100 µM hydrogen peroxide (H_2O_2) were added and left in a cold room for 5 min.Gels were left to set for 1 h at 5°C before removal of coverslips, and then slides were placed in lysis solution (2.5 M NaCl, 100 mM EDTA, 10 mM Tris, 1% Triton X-100, 10% DMSO, pH 10) for 1 h. After lysis, slides were placed in electrophoresis buffer (300 mM NaOH, 1 mM EDTA, pH 13) for 20 min of unwinding, followed by electrophoresis (25 V, 300 mA) for 20 min. Slides were washed in neutralizing buffer (0.4 M Tris-HCl, pH 7.5) and distilled water, allowed to dry overnight, and scored for % tail DNA (Leica DM4000 fluorescent microscope, 100 cells slide^{-1}; Comet Assay IV, Perceptive Instruments).

Statistical analysis

The statistical analysis for this study was performed using Excel (Microsoft Office 2007) and Statgraphics Centurion 16.1.15 (Statistical Graphics). Comet assay data (% tail DNA) were arcsine transformed before analysis. The levels of target gene expression were expressed as fold changes in larvae exposed to treatments compared with unexposed control larvae. Tests for homogeneity of variances were performed on data sets (Levene's test) before ANOVA was applied to detect significant differences in the expression of target gene and β-*actin* under different exposure conditions. Results were considered significant at $p < 0.05$.

RESULTS

SEM confirmed the nano-scale size of the nZnO (Fig. 1). However, considerable particle aggregation was observed when measuring the size distribution of nZnO in the medium using NTA over 96 h. The larger hydrodynamic diameter can be attributed to the tendency of particles to aggregate in the aqueous state (Fig. 2). ICP-OES analysis results showed that the test chamber was effective in maintaining nZnO in suspension during the 96 h exposure period. The total concentrations of nZnO remaining in suspension in the chambers were 92.5 ± 4.6%, 90.7 ± 5.1%, 62.5 ± 3.9%, 40.6 ± 6.2%, and 33.9 ± 4.5% (mean percentage at all concentrations tested), after 0, 4, 24, 48 and 96 h, respectively (Fig. 3). nZnO were dispersed in the test chambers at concentrations of 1, 5, 10, 20, 40, and 70 mg l^{-1}, and the solubility was measured by ICP-OES (Fig. 4). Although remarkable Zn^{2+} release was observed at

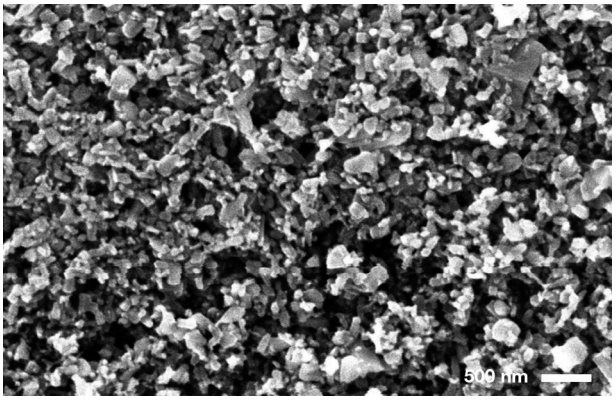

Fig. 1. Scanning electron microscopic image of zinc oxide nanoparticles. Scale bar = 500 nm

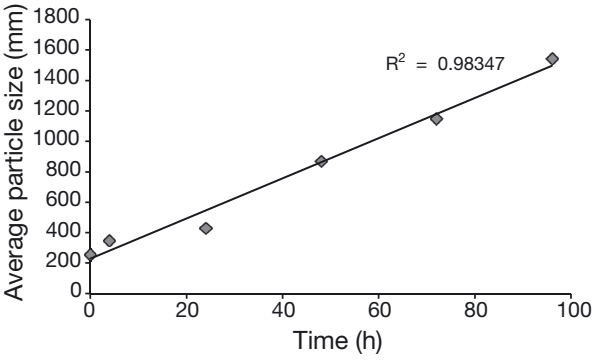

Fig. 2. Zinc oxide nanoparticles (nZnO) particle size distribution during sedimentation out of the aqueous phase at selected times (0, 4, 24, 48, 72, and 96 h). The concentration of nZnO was 1 mg l^{-1} in fish water

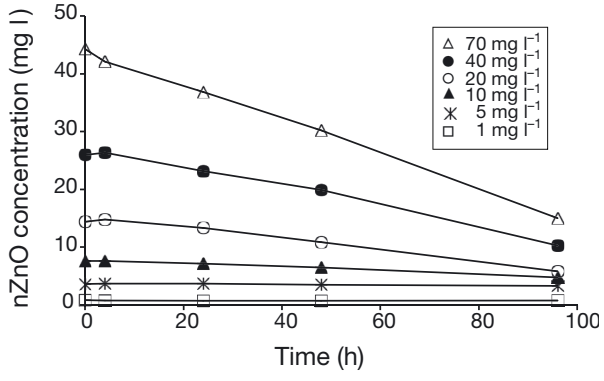

Fig. 3. Measured concentrations of zinc oxide nanoparticles (nZnO) in nanoparticle test chambers by inductively coupled plasma optical emission spectrometer during 96 h exposures. Water samples were collected for analyses during the stirring period and obtained from the middle of the chambers. To measure concentration, 1% HNO_3 was added into water samples to dissolve nZnO. Exact initial concentrations of ZnO nanoparticles were 1, 5, 10, 20, 40, and 70 mg l^{-1}

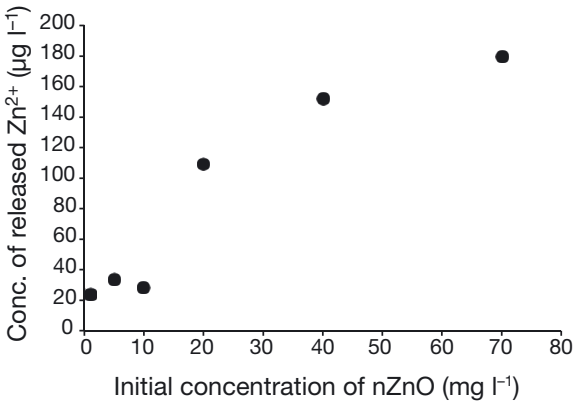

Fig. 4. Soluble zinc-releasing abilities of zinc oxide nanoparticles (nZnO) in water column. Various amounts of nZnO were dispersed in test chambers and kept for 96 h. The dispersion was then separated into particulate and soluble Zn by ultrafiltration. The amount of Zn in the filtrate (soluble Zn) was detected by inductively coupled plasma optical emission spectrometry

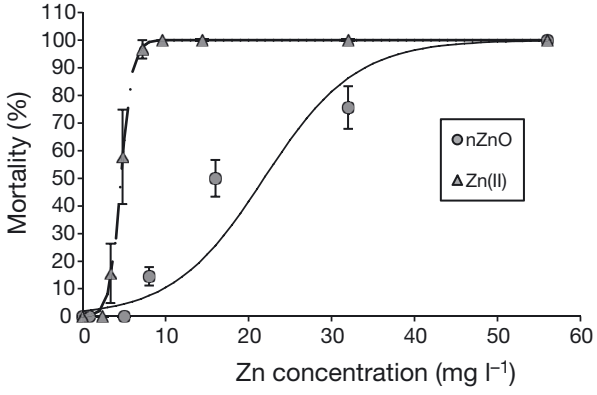

Fig. 5. Concentration response in 72 h post fertilization (hpf) zebrafish *Danio rerio* larvae exposed for 96 h to Zn, added as Zn(II) or zinc oxide nanoparticles (nZnO). There was a significant difference between Zn(II) and nZnO (data are means ± SEM; logistic regression, $p < 0.05$)

concentrations of 20 mg l^{-1} or more, Zn^{2+} release was also observed at lower concentrations.

No changes in behavior of larvae were observed after addition of nZnO or Zn(II), and there was no mortality in control larvae. Mortality increased with nZnO or Zn(II) concentrations (logistic regression, $p < 0.05$, Fig. 5). We found a statistically significant difference in acute toxicity between nZnO and Zn(II). The 96 h LC_{50} of nZnO and Zn(II) were 21.37 ± 1.81 and 4.66 ± 0.11 mg l^{-1}, respectively. Concentrations of ≤3 mg l^{-1} Zn(II) and ≤6 mg l^{-1} nZnO were selected for the sublethal Zn exposures in larval zebrafish.

Comet tail formation was observed in larval cells exposed to nZnO or Zn(II) (Fig. 6). Accordingly, nZnO and Zn(II) appeared to cause DNA damage to blood cells of the larvae. After examining the cells for the presence of comet, in the highest nZnO (6 mg l^{-1}) and Zn(II) (3 mg l^{-1}) concentrations, the mean levels of DNA damage in larvae were 25.4% and 55.3% tail DNA, respectively, and were significantly increased when compared with control values ($p < 0.05$). However, at the lowest nZnO (0.2 mg l^{-1}) and Zn(II) (0.1 mg l^{-1}) concentrations, the mean levels of DNA damage in larvae were 3.4% and 4.2% tail DNA, respectively (Fig. 7). Also, positive control H_2O_2 yielded more comet tail than nZnO or Zn(II).

The expression of β-*actin* in larvae was not affected by experimental treatments in either nZnO or Zn(II) exposure ($p > 0.05$), and therefore use of β-*actin* as a housekeeping gene was justified. Some up- and

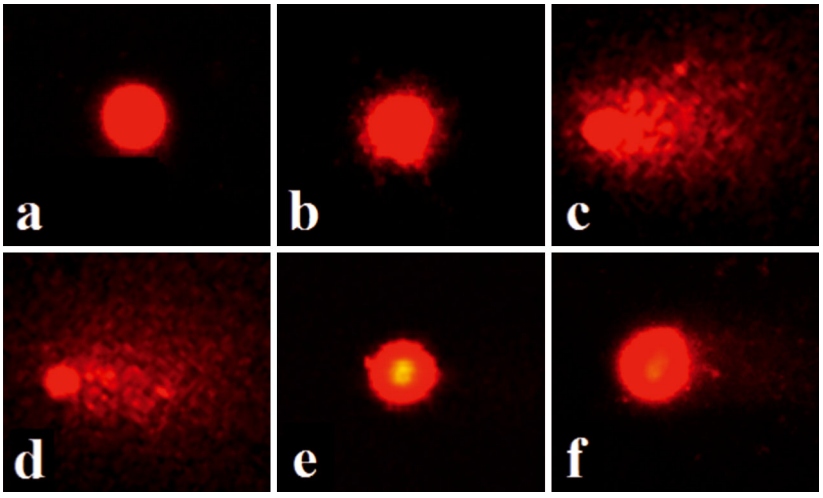

Fig. 6. Comet assay reveals DNA strand breaks in zebrafish *Danio rerio* larvae induced by Zn(II) and zinc oxide nanoparticles (nZnO) concentrations. (a) Control, (b) 0.1 mg l^{-1} Zn(II), (c) 3 mg l^{-1} Zn(II) (d) positive control with H_2O_2, (e) 0.2 mg l^{-1} nZnO, (f) 6 mg l^{-1} nZnO

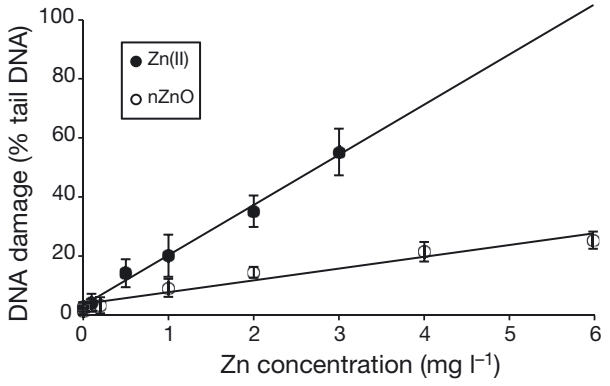

Fig. 7. DNA damage (% tail DNA, comet assay) in zebrafish *Danio rerio* larvae sampled sublethally after a 96 h exposure to aqueous Zn(II) and zinc oxide nanoparticles (nZnO). Data are mean ± SEM, $p < 0.05$

down-regulation occurred in the selected and analyzed stress-related genes (*mt2*, *rad51*, and *p53*) in larvae exposed to nZnO or Zn(II). *mt2* was significantly up-regulated when exposed to Zn(II) compared to control (Fig. 8A). We found no significant change in expression of *rad51* and *p53* genes in larvae exposed to nZnO or Zn(II) (Fig. 8B,C), whereas significant up-regulation of *mt2* occurred in larvae exposed to 2 and 3 mg l^{-1} Zn(II) (Fig. 9A). No effect of nZnO concentration on induction of genes (*mt2*, *rad51*, and *p53*) was evident in larvae exposed at 72 hpf (Fig. 9B).

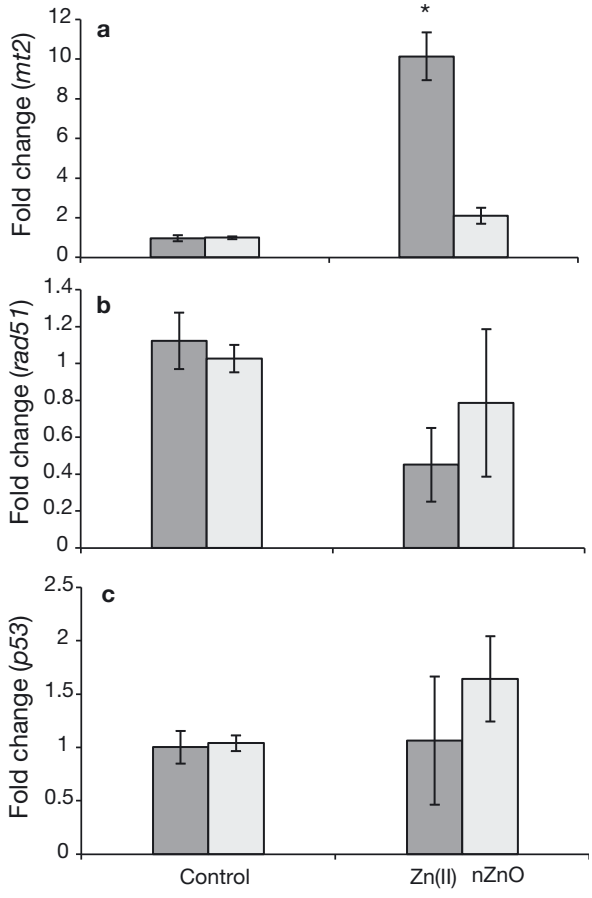

Fig. 8. Fold changes (means ± SEM) in zebrafish *Danio rerio* (a) *mt2*, (b) *rad51*, and (c) *p53* gene expression in larval zebrafish exposed (96 h) to each of Zn(II) and zinc oxide nanoparticles (nZnO) treatments. Fold changes in expression were calculated by the $2^{-\Delta\Delta Ct}$ method with target gene expression normalized to the zebrafish β-*actin* gene. *Significant induction of genes compared with control (0 mg l^{-1})

DISCUSSION

As all NPs have a very small size (<0.1 µm in diameter), they readily contaminate the environment

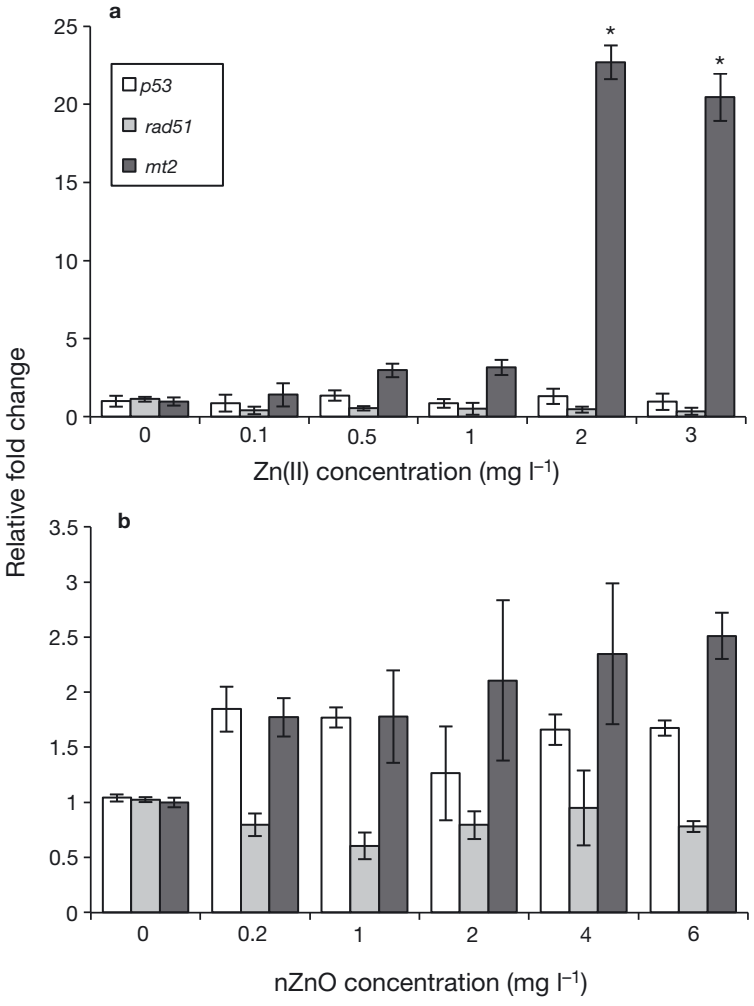

Fig. 9. Stress-related gene expression (mean ± SEM relative fold change, $2^{-\Delta\Delta Ct}$) in zebrafish *Danio rerio* larvae exposed to aqueous (a) Zn(II) and (b) zinc oxide nanoparticles (nZnO) for 96 h. *Significant induction of genes compared with control (0 mg l^{-1})

and may create a risk to humans and other organisms (Griffitt et al. 2007, Lanone et al. 2009). It is becoming increasingly important to investigate and describe possible toxicological effects associated with NPs, and to determine which particles generate the maximal potential harm to organisms in the environment. We studied the impact of nZnO on zebrafish larvae, and compared their toxicity with Zn(II), to understand the toxic mechanism of insoluble Zn by means of biomarker gene (*p53*, *rad51*, *mt2*) expression levels. Also, we investigated possible DNA strand breaks caused by Zn(II) and nZnO exposures using the comet assay.

NPs that have been tested are often dissolved in aqueous systems; this can potentially result in physicochemical property changes, e.g. agglomeration state and surface charge variation (Maynard 2002, Powers et al. 2006, Vielkind et al. 2013). Therefore, accurate characterization of NP dispersions becomes important for environmental applications and nanotoxicological investigations. Vielkind et al. (2013) characterized the state (hydrodynamic size, surface charge, and degree of agglomeration) of nZnO suspensions, and nZnO particle surface area increased dramatically as particle size decreased. This is consistent with the present study where nZnO particle concentration decreased while particle diameter and agglomeration increased over 96 h. When comparing the 96 h LC_{50} values of nZnO and Zn(II), we found that the toxicity of nZnO (96 h LC_{50}: 21.37 mg l^{-1}) was lower than that of Zn(II) (96 h LC_{50}: 4.66 mg l^{-1}) in zebrafish. This result was in accordance with previous studies on the toxicities of nZnO (96 h LC_{50}: 1.79 and 3.97 mg l^{-1}) and bulk Zn (96 h LC_{50}: 1.55 and 2.52 mg l^{-1}) (Zhu et al. 2008, Yu et al. 2011) in adult zebrafish. We hypothesized that the differences between toxicity of nZnO and Zn(II) to zebrafish larvae are due to the unusual physicochemical properties of nZnO.

Our results suggest that Zn^{2+} is an important factor in the cytotoxicity of nZnO. Generally, nZnO are classified as poorly water soluble; however, metal ion release from 'water insoluble' NPs was reported not only for ZnO but also for NiO and Cr_2O_3 NPs (Horie et al. 2009, 2013). Previous investigations suggested that nZnO showed severe cytotoxicity via Zn^{2+} release (Xia et al. 2008, Song et al. 2010). An increase in solubility is one of the important features of metal oxide NPs, and metal ion release is most important in the cytotoxicity of NPs.

An important system that controls the concentration of variable Zn(II) in cells is the metallothionein protein (MT) system. MTs control the concentration of metal ions (e.g. Zn(II)) by binding or releasing Zn when necessary (Maret 2009). They are induced by toxic metals such as silver and cadmium, or essential trace elements such as copper and Zn (Kimura & Itoh 2008). There are 4 major isoforms of *mt* genes in mammals, among which *mt1* and *mt2* function in non-neural tissues to detoxify heavy metals, regulate copper and Zn homeostasis, and restrict oxidative damage (Cho et al. 2009). In our study, Zn(II) and

nZnO showed an induction of the *mt2* gene in zebrafish larvae. Exposure to Zn(II) induced *mt2* to a greater extent (4.8-fold) than exposure to nZnO. The higher induction of *mt2* is likely to be related to the higher accumulation of Zn in zebrafish larvae. Larvae take up waterborne metals via the gills and the intestine (Minghetti et al. 2010). Expression of *rad51* and *p53* genes did not show a clear concentration-dependent response in larvae. The *p53* gene was induced up to 1.7-fold in larvae exposed to the highest nZnO concentration (6 mg l^{-1}). Larvae exposed to lower concentrations of nZnO did not have increased levels of expression of this gene, and it is possible that DNA repair mechanisms were induced earlier (Chechik & Koller 2009). DNA repair genes can be constitutively expressed in cells (Kim et al. 2001, Bladen et al. 2007) due to the importance of DNA repair on cell survival and have been used as housekeeping genes (Iwanaga et al. 2004). Therefore, the relative number of transcripts of DNA repair genes within actively dividing cells can be constantly high (Lu & King 2009), and subtle relative induction in expression could be expressive of increased levels of DNA repair activity. The *rad51* and *p53* genes investigated were induced up to about 1.5-fold, and this induction was consistent with the relatively low levels of induction observed in other studies (Reinardy et al. 2013). However, *rad51* can be highly induced in adult zebrafish, and a 32-fold change in expression has been noted in liver after a 7 d exposure to cadmium (Gonzalez et al. 2006) and 5-fold change in gills after an 8 d exposure to uranium (Lerebours et al. 2009).

DNA damage in zebrafish larvae increased with nZnO and Zn(II) exposures. In comparison, *in vitro* exposure to 20 µg ml^{-1} nZnO produced levels of DNA damage over 20% in human cells (Ng et al. 2011), as well as in zebrafish (100 mg l^{-1} exposure) with an approximate 50% increase in damage from control levels (Zhao et al. 2013). Oxidative stress induces many types of adverse effects such as protein cleavage, loss of ions, membrane peroxidation, and DNA strand breakages. Oliveira et al. (2009) showed that environmental pollutants may result in DNA damage directly by the action of parental compounds or their metabolites, or indirectly by the generated ROS. Our study demonstrated that nZnO resulted in DNA damage to larval zebrafish cells. In agreement with our results, Xiong et al. (2011) demonstrated that excessive ROS accumulation may result in increased DNA damage in the zebrafish liver.

Our study indicated that acute sub-lethal exposure to Zn(II) and nZnO can cause genotoxicity and can induce expression of stress-related genes in zebrafish larvae. To determine whether effects of nZnO are based on the free Zn(II) concentration, we exposed larval zebrafish to nZnO and to corresponding concentrations of free Zn(II) derived from $ZnCl_2$. Both nZnO and $ZnCl_2$ showed the capacity to cause DNA damage: a concentration-dependent increase in DNA strand breaks was detected in blood cells from larvae, but DNA damage was higher in response to Zn(II) than to nZnO. Induction of stress-related genes (*p53*, *rad51*, *mt2*) in larvae was complex and not directly related to nZnO and Zn(II) concentrations. The most prominent gene expression response was the induction of *mt2* in larvae exposed to Zn(II). Although the nZnO concentrations used in our present study are much higher than typical environmental exposures, our data contribute to the understanding of the potential hazards and effects of nZnO in the aquatic environment. Our results demonstrate that toxicity associated with nZnO is primarily due to the release of Zn(II).

Acknowledgements. This project was funded by Recep Tayyip Erdoğan University, Scientific Research Projects Fund (Project No: 2013.103.01.4). We thank H. Turker Akcay and Murat Sirin for technical assistance with ICP-OES, SEM, and NTA.

LITERATURE CITED

Bai W, Zhang Z, Tian W, He X, Ma Y, Zhao Y, Chai Z (2010) Toxicity of zinc oxide nanoparticles to zebrafish embryo: a physicochemical study of toxicity mechanism. J Nanopart Res 12:1645–1654

Bladen CL, Navarre S, Dynan WS, Kozlowski DJ (2007) Expression of the Ku70 subunit (XRCC6) and protection from low dose ionizing radiation during zebrafish embryogenesis. Neurosci Lett 422:97–102

Blinova I, Ivask A, Heinlaan M, Mortimer M, Kahru A (2010) Ecotoxicity of nanoparticles of CuO and ZnO in natural water. Environ Pollut 158:41–47

Boran H, Boyle D, Handy RD, Altinok I, Henry TB (2012) Development of a test chamber to enable homogenous aqueous phase dispersions of nanoparticles for testing nanoparticle toxicity in fish. In: 6th SETAC World Congress 2012, SETAC Europa 22nd Annual Meeting, 20–24 May, Berlin. SETAC Europe, Brussels

Boyle D, Boran H, Atfield AJ, Henry TB (2015) Use of an exposure chamber to maintain aqueous phase nanoparticle dispersions for improved toxicity testing in fish. Environ Toxicol Chem 34:583–588

Buerki-Thurnherr T, Xiao L, Diener L, Arslan O and others (2013) In vitro mechanistic study towards a better understanding of ZnO nanoparticle toxicity. Nanotoxicology 7: 402–416

Buffle J, Altmann RS, Filella M, Tessier A (1990) Complexation by natural heterogeneous compounds: site occupation distribution functions, a normalized description of metal

complexation. Geochim Cosmochim Acta 54:1535–1553

Chechik G, Koller D (2009) Timing of gene expression responses to environmental changes. J Comput Biol 16: 279–290

Cho YS, Lee SY, Kim KY, Nam YK (2009) Two metallothionein genes from mud loach *Misgurnus mizolepis* (Teleostei; Cypriniformes): gene structure, genomic organization, and mRNA expression analysis. Comp Biochem Physiol B Biochem Mol Biol 153:317–326

Franklin NM, Rogers NJ, Apte SC, Batley GE, Gadd GE, Casey PS (2007) Comparative toxicity of nanoparticulate ZnO, bulk ZnO, and $ZnCl_2$ to a freshwater microalga (*Pseudokirchneriella subcapitata*): the importance of particle solubility. Environ Sci Technol 41:8484–8490

Gonzalez P, Baudrimont M, Boudou A, Bourdineaud JP (2006) Comparative effects of direct cadmium contamination on gene expression in gills, liver, skeletal muscles and brain of the zebrafish (*Danio rerio*). Biometals 19: 225–235

Gottschalk F, Sonderer T, Scholz RW, Nowack B (2009) Modeled environmental concentrations of engineered nanomaterials (TiO_2, ZnO, Ag, CNT, fullerenes) for different regions. Environ Sci Technol 43:9216–9222

Griffitt RJ, Weil R, Hyndman KA, Denslow ND, Powers K, Taylor D, Barber DS (2007) Exposure to copper nanoparticles causes gill injury and acute lethality in zebrafish (*Danio rerio*). Environ Sci Technol 41:8178–8186

Horie M, Nishio K, Fujita K, Kato H and others (2009) Ultrafine NiO particles induce cytotoxicity *in vitro* by cellular uptake and subsequent Ni(II) release. Chem Res Toxicol 22:1415–1426

Horie M, Nishio K, Endoh S, Kato H and others (2013) Chromium (III) oxide nanoparticles induced remarkable oxidative stress and apoptosis on culture cells. Environ Toxicol 28:61–75

Hyung H, Fortner JD, Hughes JB, Kim JH (2007) Natural organic matter stabilizes carbon nanotubes in the aqueous phase. Environ Sci Technol 41:179–184

Iwanaga R, Komori H, Ohtani K (2004) Differential regulation of expression of the mammalian DNA repair genes by growth stimulation. Oncogene 23:8581–8590

Kim GW, Noshita N, Sugawara T, Chan PH (2001) Early decrease in DNA repair proteins, Ku70 and Ku86, and subsequent DNA fragmentation after transient focal cerebral ischemia in mice. Stroke 32:1401–1407

Kimura T, Itoh N (2008) Function of metallothionein in gene expression and signal transduction: newly found protective role of metallothionein. J Health Sci 54:251–260

Lanone S, Rogerieux F, Geys J, Dupont A and others (2009) Comparative toxicity of 24 manufactured nanoparticles in human alveolar epithelial and macrophage cell lines. Part Fibre Toxicol 6:14

Lerebours A, Gonzalez P, Adam C, Camilleri V, Bourdineaud JP, Garnier-Laplace J (2009) Comparative analysis of gene expression in brain, liver, skeletal muscles, and gills of zebrafish (*Danio rerio*) exposed to environmentally relevant waterborne uranium concentrations. Environ Toxicol Chem 28:1271–1278

Li S, Pan X, Fan ZY, Wallis LK, Chen ZL, Diamond SA (2014) Comparison of the phototoxicity of TiO_2 nanoparticle and graphene-TiO_2 nanoparticle composite in *Daphnia magna* and *Oryzias latipes.* Chemosphere 112:62–69

Lu C, King RD (2009) An investigation into the population abundance distribution of mRNAs, proteins, and metabolites in biological systems. Bioinformatics 25:2020–2027

Ma H, Williams PL, Diamond SA (2013) Ecotoxicity of manufactured ZnO nanoparticles—a review. Environ Pollut 172:76–85

Maret W (2009) Molecular aspects of human cellular zinc homeostasis: redox control of zinc potentials and zinc signals. Biometals 22:149–157

Maynard AD (2002) Experimental determination of ultrafine TiO_2 deagglomeration in a surrogate pulmonary surfactant: preliminary results. Ann Occup Hyg 46(Suppl 1): 197–202

Minghetti M, Leaver MJ, George SG (2010) Multiple Cu-ATPase genes are differentially expressed and transcriptionally regulated by Cu exposure in sea bream, *Sparus aurata*. Aquat Toxicol 97:23–33

Nel A, Xia T, Mädler L, Li N (2006) Toxic potential of materials at the nanolevel. Science 311:622–627

Ng KW, Khoo SPK, Heng BC, Setyawati MI and others (2011) The role of the tumor suppressor p53 pathway in the cellular DNA damage response to zinc oxide nanoparticles. Biomaterials 32:8218–8225

Oliveira M, Maria VL, Ahmad I, Serafim A, Bebianno MJ, Pacheco M, Santos MA (2009) Contamination assessment of a coastal lagoon (Ria de Aveiro, Portugal) using defence and damage biochemical indicators in gill of *Liza aurata*—an integrated biomarker approach. Environ Pollut 157:959–967

Pfaffl MW (2001) A new mathematical model for relative quantification in real-time RT-PCR. Nucleic Acids Res 29:e45

Powers KW, Brown SC, Krishna VB, Wasdo SC, Moudgil BM, Roberts SM (2006) Research strategies for safety evaluation of nanomaterials. Part VI. Characterization of nanoscale particles for toxicological evaluation. Toxicol Sci 90:296–303

Regoli F, Principato G (1995) Glutathione, glutathione-dependent and antioxidant enzymes in mussel, *Mytilus galloprovincialis*, exposed to metals under field and laboratory conditions: implications for the use of biochemical biomarkers. Aquat Toxicol 31:143–164

Reinardy HC, Dharamshi J, Jha AN, Henry TB (2013) Changes in expression profiles of genes associated with DNA repair following induction of DNA damage in larval zebrafish *Danio rerio.* Mutagenesis 28:601–608

Sharma V, Anderson D, Dhawan A (2012) Zinc oxide nanoparticles induce oxidative DNA damage and ROS-triggered mitochondria mediated apoptosis in human liver cells (HepG2). Apoptosis 17:852–870

Shaw BJ, Handy RD (2011) Physiological effects of nanoparticles on fish: a comparison of nanometals versus metal ions. Environ Int 37:1083–1097

Song W, Zhang J, Guo J, Zhang J, Ding F, Li L, Sun Z (2010) Role of the dissolved zinc ion and reactive oxygen species in cytotoxicity of ZnO nanoparticles. Toxicol Lett 199:389–397

US EPA (United States Environmental Protection Agency) (2007) Nanotechnology White Paper. EPA 100/B-07/001. Science Policy Council, US Environmental Protection Agency, Washington, DC

Vielkind M, Kampen I, Kwade A (2013) Zinc oxide nanoparticles in bacterial growth medium: optimized dispersion and growth inhibition of *Pseudomonas putida.* Adv Nanopart 2:287–293

Wilson M, Hogstrand C, Maret W (2012) Picomolar concentrations of free zinc(II) ions regulate receptor protein-tyrosine phosphatase β activity. J Biol Chem 287:9322–9326

Wong S, Leung P, Djurišic A, Leung K (2010) Toxicities of nano zinc oxide to five marine organisms: influences of aggregate size and ion solubility. Anal Bioanal Chem 396:609–618

Xia T, Kovochich M, Liong M, Mädler L and others (2008) Comparison of the mechanism of toxicity of zinc oxide and cerium oxide nanoparticles based on dissolution and oxidative stress properties. ACS Nano 2:2121–2134

Xiong D, Fang T, Yu L, Sima X, Zhu W (2011) Effects of nano-scale TiO_2, ZnO and their bulk counterparts on zebrafish: acute toxicity, oxidative stress and oxidative damage. Sci Total Environ 409:1444–1452

Yu LP, Fang T, Xiong DW, Zhu WT, Sima XF (2011) Comparative toxicity of nano-ZnO and bulk ZnO suspensions to zebrafish and the effects of sedimentation, •OH production and particle dissolution in distilled water. J Environ Monit 13:1975–1982

Zhao X, Wang S, Wu Y, You H, Lv L (2013) Acute ZnO nanoparticles exposure induces developmental toxicity, oxidative stress and DNA damage in embryo-larval zebrafish. Aquat Toxicol 136-137:49–59

Zhou D, Keller AA (2010) Role of morphology in the aggregation kinetics of ZnO nanoparticles. Water Res 44: 2948–2956

Zhu X, Zhu L, Duan Z, Qi R, Li Y, Lang Y (2008) Comparative toxicity of several metal oxide nanoparticle aqueous suspensions to zebrafish (*Danio rerio*) early developmental stage. J Environ Sci Health Part A Toxic-Hazard Subst Environ Eng 43:278–284

Zhu X, Wang J, Zhang X, Chang Y, Chen Y (2009) The impact of ZnO nanoparticle aggregates on the embryonic development of zebrafish (*Danio rerio*). Nanotechnology 20:195103

Zimmermann YS, Schäffer A, Hugi C, Fent K, Corvini PFX, Lenz M (2012) Organic photovoltaics: potential fate and effects in the environment. Environ Int 49:128–140

Editorial responsibility: Thomas Braunbeck, Heidelberg, Germany

Submitted: May 4, 2015; Accepted: October 27, 2015
Proofs received from author(s): December 10, 2015